Characterization of the incorporation of a granular medium into elastomer matrices during mixing process

Nikhil Tembhurnikar, Jean-Charles Majesté, Sylvain Martin, Olivier Bonnefoy

Characterization of the incorporation of a granular medium into elastomer matrices during mixing process

Nikhil Tembhurnikar[1], Jean-Charles Majesté[1], Sylvain Martin[2], Olivier Bonnefoy[2]

1 Université de Lyon, F-42023, Saint-Etienne, France; CNRS, UMR 5223, Ingénierie des Matériaux Polymères, F-42023, Saint-Etienne, France; and Université de Saint-Etienne, Jean Monnet, F-42023, Saint Etienne, France

2 Mines Saint-Etienne, Univ Lyon, CNRS, UMR 5307 LGF, Centre SPIN, F-42023, Saint-Etienne, France

Abstract

Mixing of filler particles with elastomers is one of the most important steps in tire manufacturing process. Precipitated Silica (Si), as a filler, shows enhanced propertiescompared to carbon black (CB) when incorporated with an elastomer such as low rolling resistance, high wet grip performance and high wear resistance. According to the standard rubber mixing process, the fragmentation of the filler particles in an elastomer during mixing must yield to breakage of particles to a size that enables homogenous mixing of the material. Hence, this experimental study is concerned with understanding the behavior of silica during its incorporation in the elastomer. Incorporation is done through shear forces present in the Internal Mixer. Different experimental methodologies are used to measure the particle sizedistribution. For free silica particles that have been fragmented but not incorporated, we use Laser granulometry. Silica embedded in elastomer is analyzed using X-ray tomography. The results obtained suggest that free silica and silica embedded in elastomer follow erosion mechanism.

1. Introduction

The tread part of the tire, which is in contact with the road surface, largely depends on key tire characteristics like wear resistance, abrasion resistance and rolling resistance[1]. Generally, elastomers like styrene butadiene rubber (SBR), butadiene rubber (BR), natural rubber (NR), etc. are mixed with processing oils, additives, coupling agents, accelerators, and filler particles. Addition of filler particles like silica (Si) or carbon black (CB) reinforces the elastomers and improves its wear resistance. Carbon black (CB) is the most commonly used filler particle, mainly due to its affinity towards natural rubber (NR). In mid 90s, Rauline came up with a concept called as "Green tires"[2], where precipitated silica (Si) was used as a filler. Silica provides a better compromise of low rolling resistance, high wet grip performance and high wear resistance[3] than carbon black. On the other hand, when silica is mixed with elastomer, its dispersion is poor, mainly due to the great difference between the surface polarities of silica and elastomer[4,5]. Silica tends to agglomerate easily due to hydrogen bonding[6,7] and thus, chain-like structures can be easily formed. Coupling agents like Bis-(triethoxysilylpropyl) tetrasulfide (TESPT) reduce the surface polarities but the distribution is still not satisfactory as compared to carbon black (CB). The advantages of silica will be effective only when particles are homogeneously distributed throughout the elastomer.

In a classical industrial production line, the mixing of filler particles and elastomer is composed of three stages: 1) Incorporation – Filler particles are mixed with elastomer to form a coherent mass. At the end of this step, most of the filler particles are in the form of agglomerates embedded in elastomer. 2) Dispersion - Filler agglomerates (0.2-30 µm) are broken down to the size of the aggregates (50-500 nm[8] and 3) Distribution - It corresponds to mixing in a usual sense, that it is homogenization on macro scale[9–11].

Mixing of Si and SBR in an internal mixer has been studied extensively mostly with the objective of improving its dispersion process. Majesté and Vincent[12] used SBR and silica by premixing the rubber in an internal mixer and then adding silica and coupling agents like TESPT to understand the filler-filler and filler-rubber interactions during the dispersion process and also its impact on the final structure of silica. Kaewsakul et al[13] studied mixing conditions of silica reinforced natural rubber (NR) by adding silica and TESPT in two steps (masticated NR mixed with half of silica and TESPT for half of the mixing time followed by adding the other half for the remaining mixing

time) in an internal mixer. They deduced that the viscosity increased with dump (end) temperature from 100 to 150°C, indicating the occurrence of cross-linking of NR due to sulfur present in TESPT. Ramier[14] et al mixed Z1165 MP silica and SBR in a three-step mixing process to evaluate the influence of filler surface modification on the payne effect in silica filled SBR. In the first step, SBR is added along with the incorporation of silica into SBR. Surface treatment such as Stearic acid is also added in the same step. The silica is dispersed and desagglomerated during this step. The second step includes in addition of ZnO which is important for vulcanization step. The second step optimizes the dispersion occurred during the first step. The third step involves in incorporating the vulcanization system and the temperature of mixing is at 150°C. Quite recently, Jin[15] studied the dispersion of silica in SBR to understand filler-filler interaction, filler-polymer coupling via silane and formation of additional crosslinks due to the release of free sulfur from silane. The mixing was done using two step procedure.

All these studies try to understand the dispersion mechanism of silica in SBR in an internal mixer using several mixing steps but little to no attention has been given to the initial stage of mixing. The fragmentation mechanism plays an important part in understanding the incorporation process of highly dispersible silica into styrene butadiene rubber. Basically, there are three types of fragmentation mechanisms. Rupture mechanism[16–18] is reserved for breakage patterns in which clear fracture planes (cracks) are visible. This mode produces two or more large daughter fragments and is normally accompanied by some fines production adjacent to the impact site. The erosion mechanism[19–21] is characterized by the detachment of small fragments from the outer surface of the agglomerate and the disintegration mechanism[22] corresponds to the creation of many small fragments in a short period of time. All these studies perform shear mixing of silica and SBR in different steps to investigate the poor dispersion process but the data on the initial stages of mixing (incorporation) is scarce.

Because it has been sparsely addressed, this article emphasizes on the initial stage of silica and elastomer mixing (incorporation) that includes understanding the time evolution of silica particle size distribution. The incorporation process of silica and SBR is studied to identify the mechanisms that control the passage of a heterogeneous mixture on the macroscopic scale to a homogeneous mixture at the microscopic scale. Single step mixing of silica and SBR is done to observe the behavior of both free silica and silica embedded in SBR simultaneously.

2. Materials

Solution Styrene Butadiene Rubber (S-SBR) providedby Michelin is used as a matrix. It contains 25% styrene, 58% butadiene (trans 1,2 form) and 17% butadiene (trans 1,4 form). SBR has a density of 0.938 g/cm^3 at room temperature and the glass transition temperature is -30°C. Its molecular weight is 310 000 g/mol[23].

The filler used is a highly dispersible precipitated silica (Zeosil Z1165 MP) produced by Solvay[24]. The initial particle size distribution of silica micro-pearls before mixing is determined with the help of laser granulometry as shown in Figure 1. The median diameter is 252 µm. The span (d_{90}-d_{10}/d_{50}) is 1.4 which is used to determine the width of the size distribution where d_{90}, d_{10} and d_{50}-90%, 10% and 50% of the total volume of the material in the sample contained.

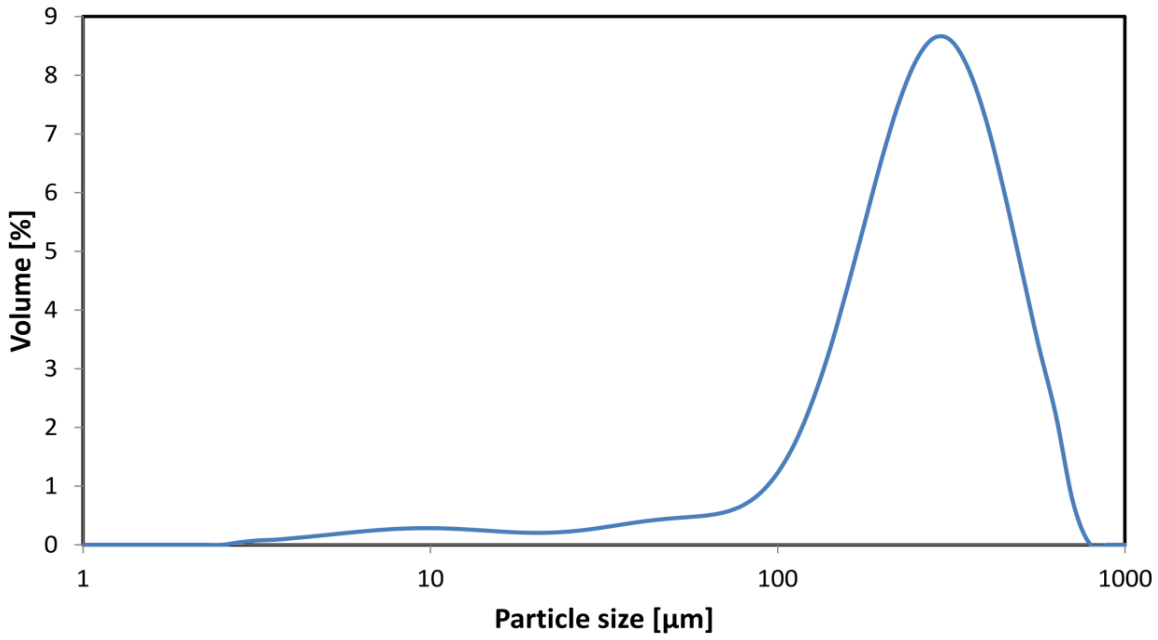

Figure 1. PSD of silica micro-pearls before mixing

The experimental setup consists in a Rheomix Haake 600 internal mixer, with 50 cm^3 volume (used at 70% filling rate). The mixer consists of two counter rotating roller rotors with slight speed differential (ratio 2/3). The shearing action occurs between the rotors and the cylinder and between the rotors themselves. Ram is used to exert and control pressure on the sample during the experimentation. Discharge of the batch occurs at the bottom of the mixing chamber (see Figure 2). The internal mixer is operated at 50°C.

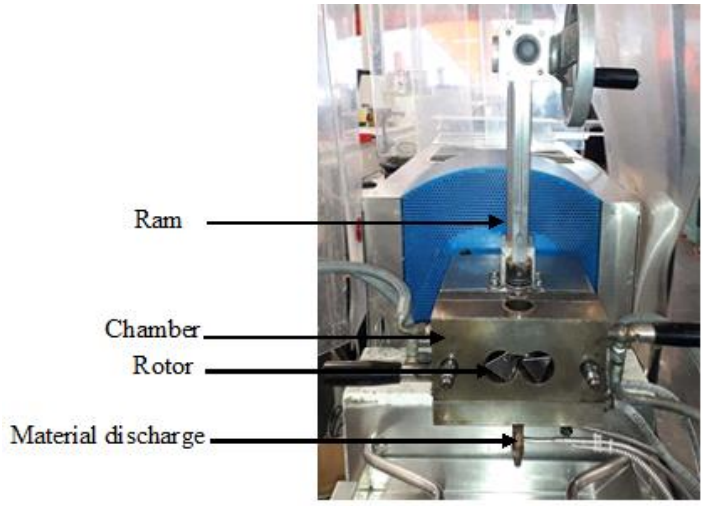

Figure 2. Internal mixer (Rheomix Haake 600)

3. Experimental Procedure

To mimic the industrial process as close as possible, instead of adding silica into SBR step by step, they are introduced all at once in the internal mixer before starting the experiments. SBR is cut into small pieces of approximately 1 cm^3 and added at the bottom of the chamber followed by silica particles on top. The parameters investigated and their values are indicated in Table 1

Table 1. Investigated parameters

Rotational speed ω [rpm]	5, 10, 20, 60, 100
Mixing time t [s]	30, 60, 90, 120, 150, 180, 240, 300
Weight fraction of silica (x_0) [%]	10, 20, 25

For the filler loads x_0=10%, 20% and 25%, and for every rotational speed, eight experiments are performed with mixing times up to 300 s. After mixing is completed, free silica and SBR in which silica is embedded are collected separately.

Free silica particles are analyzed, in the form of particle size distribution, using Laser granulometry. The Malvern Mastersizer 2000 uses the physics of scattering light where particles are passed through a focused laser beam. These particles scatter light at an angle that is inversely proportional to their size. The map of scattering intensity versus angle is the primary source of information used to calculate the particle size. The characterization can be performed using two methods: dry air and wet methods. In our study, wet method without ultrasound is applied because it does not fragment the silica particles and because a lesser amount of silica particles is required

to perform the measurement.

Characterization of embedded silica has been performed using X-Ray tomography technic. SBR containing silica is cut in cubic samples of 10 mm and analyzed using a Nanotom 180 X-Ray Tomograph (XRT) with an acceleration voltage of 75 kV and a current of 200 µA (tungsten target). A total of 2000 projections of 2304 x 2304 pixels is acquired with 500 ms integration time and subsequently reconstructed. The 3D images obtained have a voxel size of 8 µm.

The image analysis procedure performed with Avizo 5.2 software is as follows:

- **Thresholding**: It is a binarization step where 1 is assigned to silica and 0 to SBR. All the SBR matrix is discarded.
- **Opening:** To avoid the inclusion of SBR matrix and obtain only silica particles, an opening step is performed. Since the voxel size is 8 µm, the objects smaller than 20-30 µm are impossible to detect. This step removes all the rubber chunks along with silica particles below 25 µm.
- **Label Analysis:** This step labels every silica particle. This step also gives the values of parameters like the equivalent diameter, sphericity, volume of every silica particle.
- **Volume Rendering:** Avizo has the ability to enlarge the image into 3D using volume rendering tool, which shows only silica particles inside SBR.

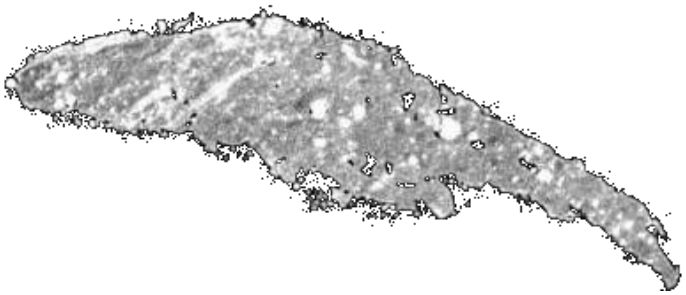

1. Initial Image (grey level)

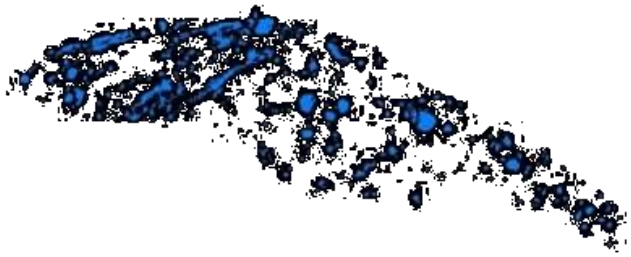

2.Thresholding

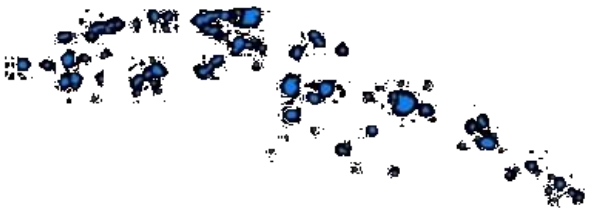

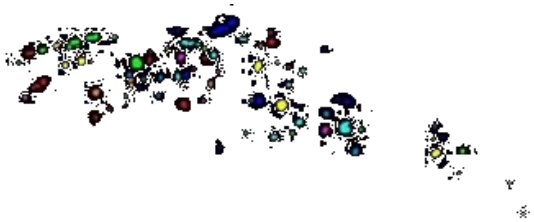

3. Opening 4. Label Analysis

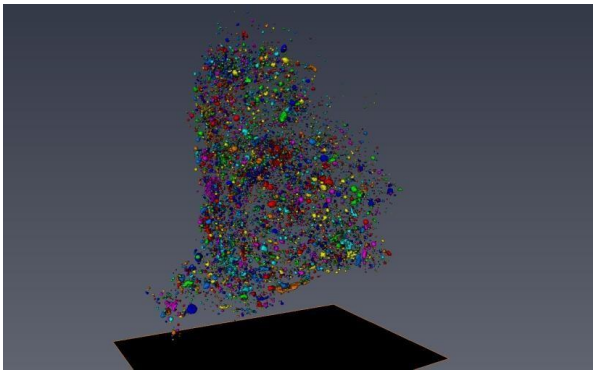

5. Volume rendering showing that the SBR sample is uniformly filled with silica particles.

Figure 3. Image analysis (The size of the four bounding boxes is 11.12 mm x 7.12 mm)

4. Results and discussion:

The results obtained from analyzing both free silica and silica embedded in the SBR samples are presented in detail in this section.

4.1. Free Silica

4.1.1. Incorporation rate

The incorporation rate can be estimated by measuring the amount of leftover free flowing silica (as opposed to silica particles embedded in SBR) after mixing. For an initial particle load of x_0=20 wt%, Figure 4 shows the time evolution of the fraction of free silica defined as mass fraction equation:

$$\Psi = \frac{\text{mass of free flowing silica}}{\text{Initial mass of silica}}$$

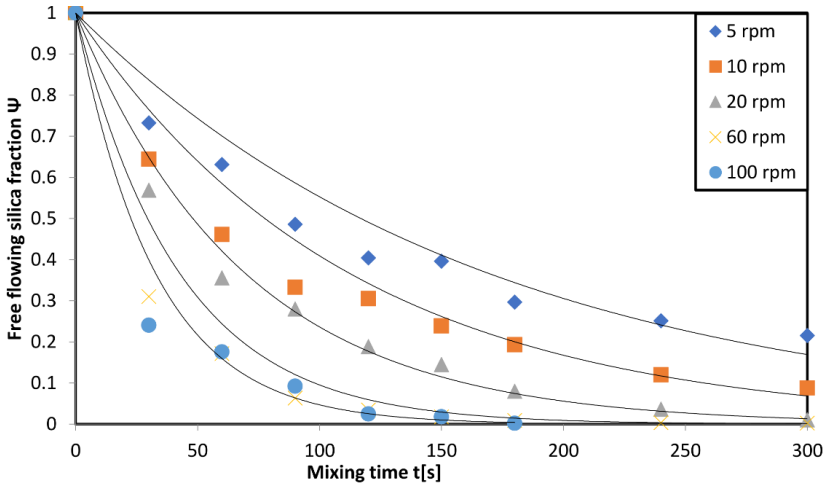

Figure 4. Time evolution of free silica fraction at different rotational speeds for initial silica load of 20 wt%

Figure 4 shows that the free silica fraction decreases exponentially with the mixing time, irrespective of the rotational speed. Using a least-squares regression, each curve is approximated by an exponential law $\Psi = A.\exp\left(\frac{-t}{\tau}\right)$ where t is mixing time (s) and τ a characteristic time. The rate of incorporation (R = 1/τ) is plotted against the rotational speed (Figure 5). The graph shows that R is proportional to the square root of the rotational speed. Hence, the incorporation process is well described by:

$$\Psi = \exp(-R.t) \text{ where } R = k.\sqrt{\omega}$$

The constant k at 20 wt% is found to be 3.0 10^{-3} (1/s). We can see that the rotor speed plays a very important role in the behavior of free silica during mixing. This was identified by Campanelli[26] using different sizes of carbon black. In contrast to our results, they concluded that the incorporation rate has a linear dependency on the rotor speed. Like us, he also specified that the size reduction process is represented by a first order rate equation.

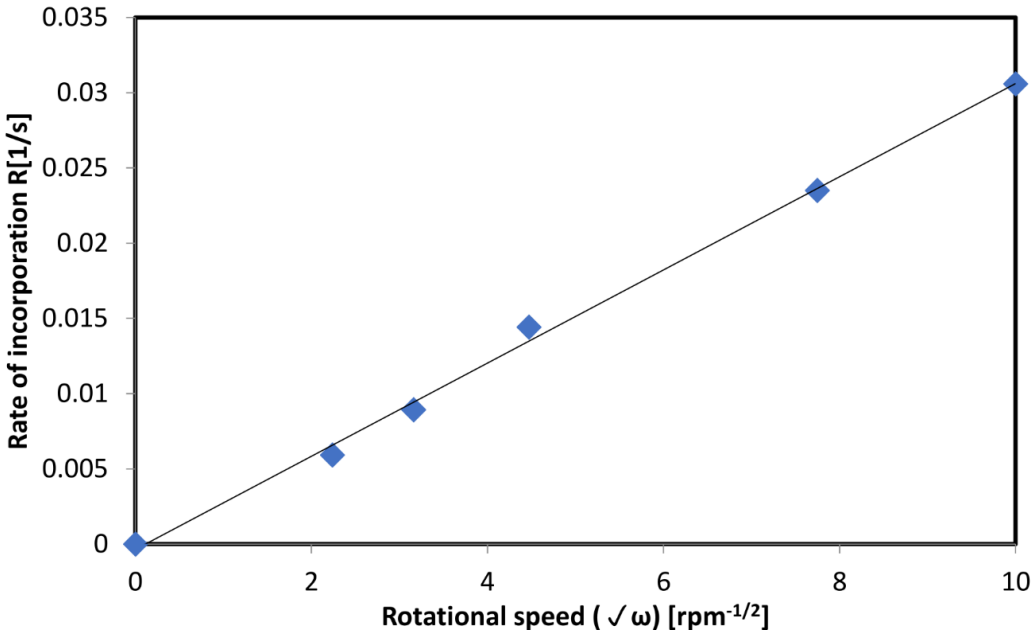

Figure 5. Rate of incorporation as a function of the rotational speed ω for x_0 = 20 wt%

4.1.2. Fragmentation rate

The particle size distribution of free flowing silica after mixing at 10 rpm for different mixing times and for x_0 = 20 wt% is shown in Figure 6.

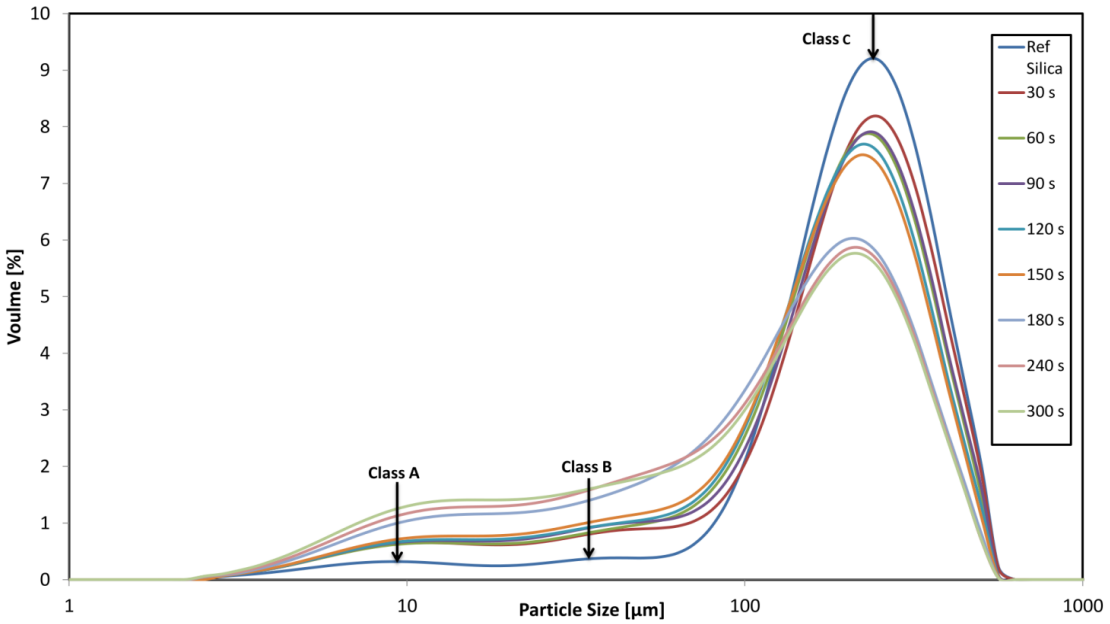

Figure 6. PSD of free silica after different mixing times for ω=10 rpm, x_0=20 wt%

The PSD clearly suggests that three populations of silica particles are co-existing. Class A and Class B show that the large clusters of silica from Class C are decomposed into small clusters at 10 µm and 40 µm respectively. The three classes or the peaks are separated by graph deconvolution with the help of fityk software as shown in Figure 7. After deconvolution is done, Classes A, B and C are separated which helps in determining their PSDs.

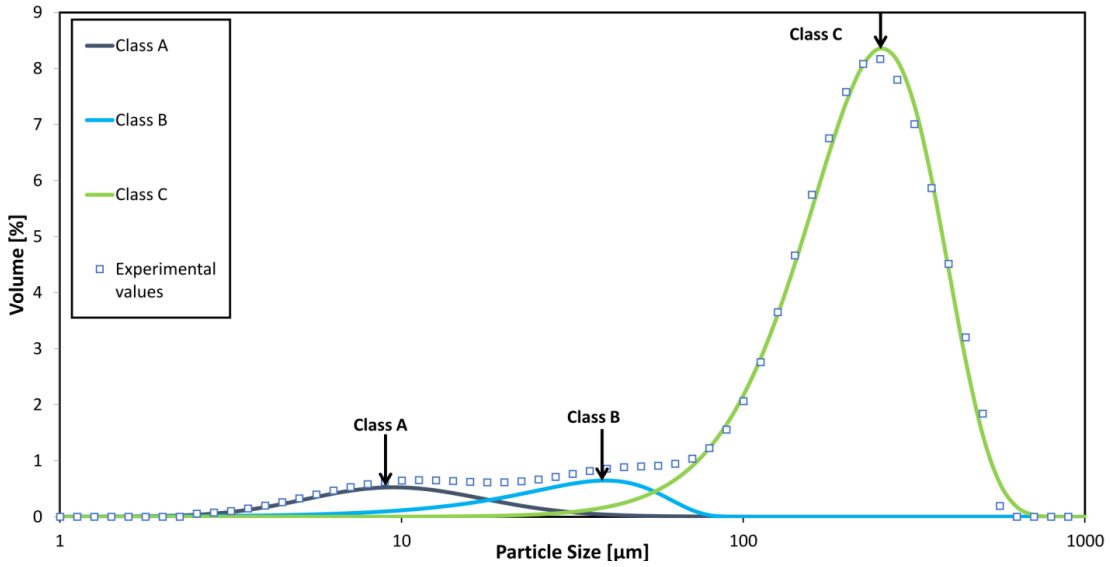

Figure 7. PSD decomposition example for ω=10 rpm and x_0=20 wt%

Each PSD is considered as the sum of three log-normal distributions. A parameter identification is performed by a least square regression method using Fityk solver. A total of five independent parameters are obtained for each PSD:

x^A, x^B, d_p^A, d_p^B and d_p^C where:

x^A – Volume fraction of class A

x^B – Volume fraction of class B

d_p^A – peak diameter of class A

d_p^B- peak diameter of class B

d_p^C - peak diameter of class C

The volume fraction x^A of particles belonging to class A is equal to the surface under the black curve. By definition, the volume fraction x^C can be calculated as $x^C=1-x^A-x^B$. The results of the unconstrained optimization show that the peak diameters d_p of classes A and B are nearly constants. They range between 8 and 12 µm for class A and 36 and 50 µm for class B, for all PSDs. Hence, a constrained optimization is done with $d_p^A=10$ µm and $d_p^B=40$ µm. It makes the interpretation of the PSDs easier because now just three values (x^A, x^B and d_p^C) are analyzed instead of five.

The values of x^A and x^B are plotted against the mixing time for all the rotational speeds (Figure 8) for $x_0=20$ wt%. The figure shows that there is a global increase in the volume fraction of class A and class B particles, for all the rotational speeds. The data is scattered but show a similar evolution for classes A and B: the increase is sharp at low mixing time (up to 150 s) and then the values show signs of plateauing as the mixing times increases. For class A, the volume fraction changes from 4.5% at t=0 to between 9% and 15% at 150 s mixing time. For class B, the volume fraction changes from 1.8% at t=0 to between 5% and 14% at 150 s.

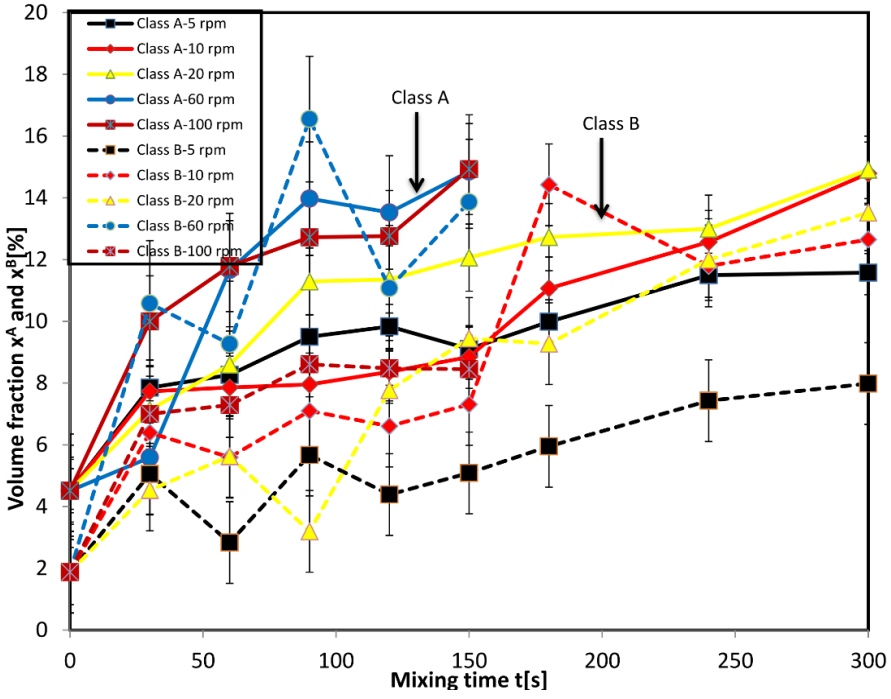

Figure 8. Time evolution of class A (dotted lines) and class B (solid line) volume fractions for $x_0=20$ wt%

In Figure 9, the peak diameter d_p^c of large particles is plotted against the mixing time for all rotational speeds. It is observed that the particle size decreases almost linearly with the rotational speed. As the rotational speed increases, the decrease in the particle size is steeper. At 100 rpm, and after 150 s, the peak diameter of the class C is reduced by 31%. The linearity in the particle size reduction indicates that in Z1165 MP silica, continuous detachment of large granules into small fragments has occurred. Hence, it can be deduced that the main mechanism of fragmentation of free-flowing silica is erosion. Rwei et al[20] determined that if the kinetics of particle size reduction follow the first order rate equation, then the particles undergo erosion mechanism which is consistent with the results obtained in Figure 5.

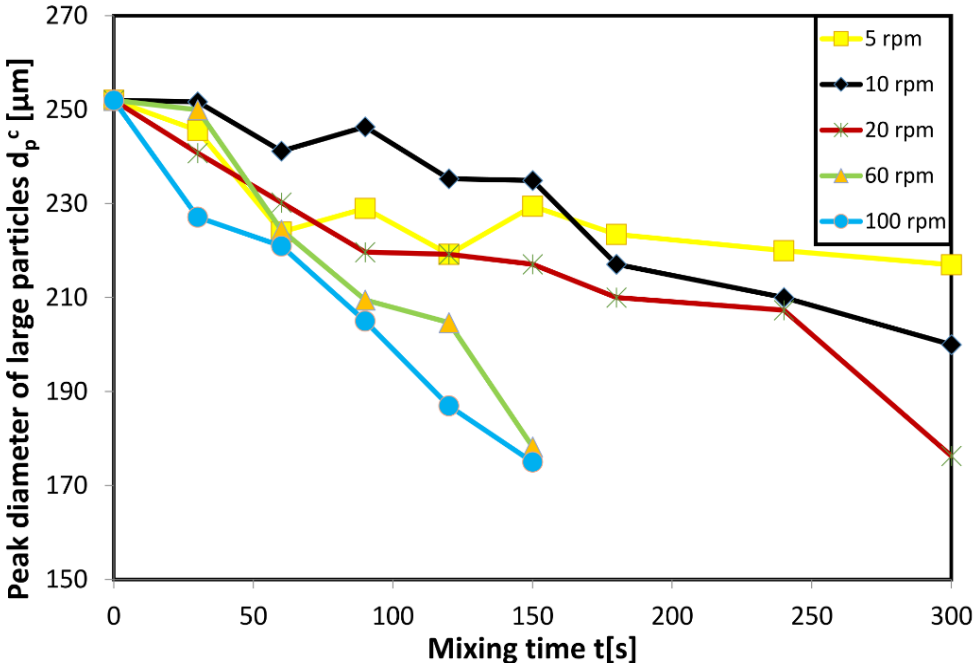

Figure 9. Peak diameter of free large particles (classC) as a function of mixing time for x_0=20 wt%

4.1.3. Influence of the initial filler load

Similar experiments were done at different initial weight fractions of silica (10 wt% and 25 wt%) at 10 rpm to check whether the behavior is the same. Figure 10 and Figure 11 show the particle size distribution graph at 10 and 25 wt% respectively at 10 rpm. By comparing figures 6, 10 and 11, it can be determined that the PSD decreases rapidly if the filler concentration is less. The figures show that the PSD changes more rapidly for x_0=10 % followed by x_0=20 % and then little change in x_0=25 %.

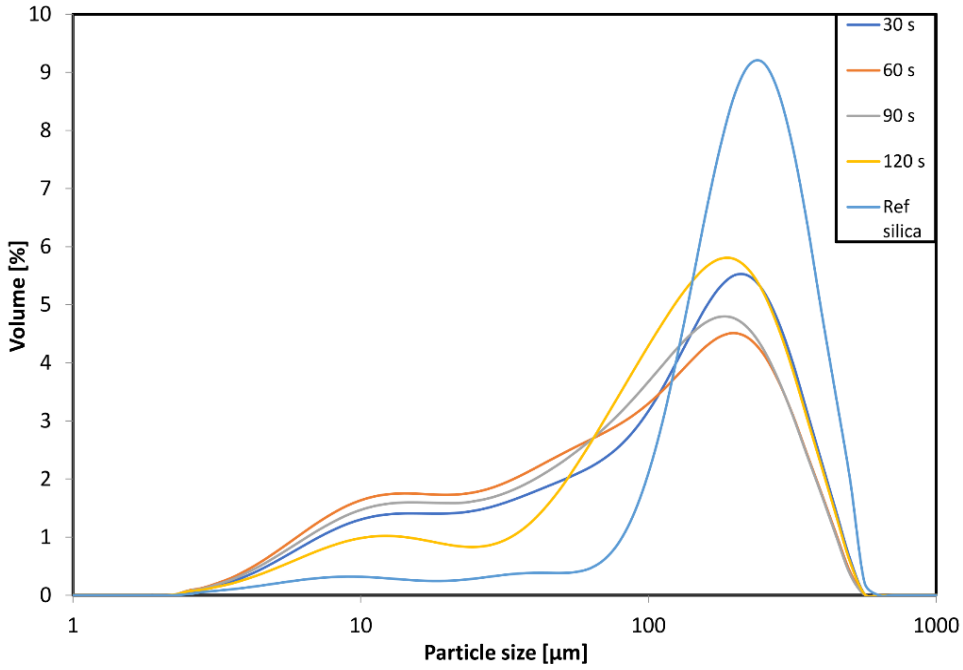

Figure 10. PSD of free silica at different mixing time for ω=10 rpm and x_0=10 wt%

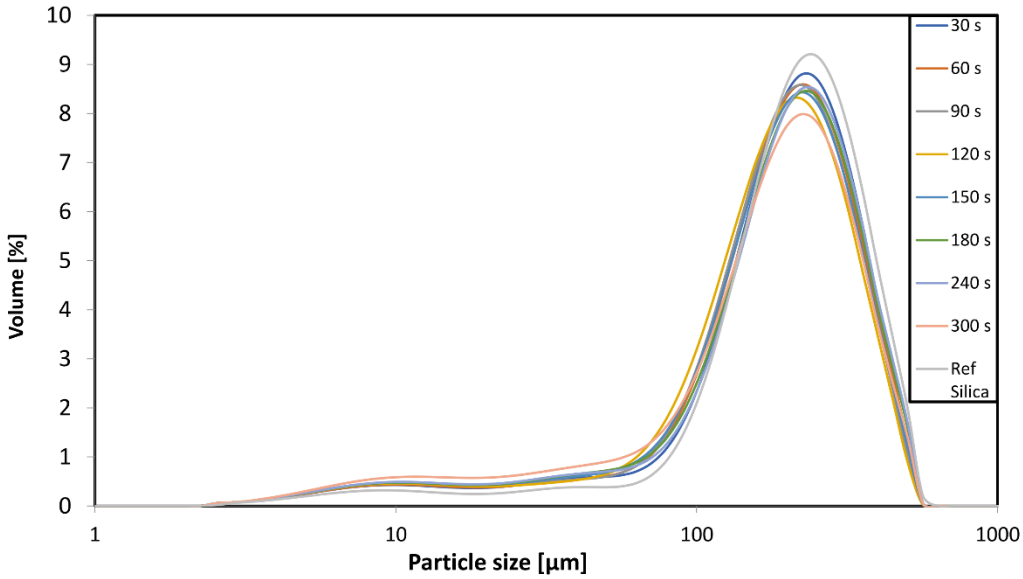

Figure 11. PSD of free silica at different mixing time for ω=10 rpm, x_0=25wt%

Figure 12 shows the time evolution of free silica at x_0=10 wt%, 20 wt% and 25 wt% respectively at 10 rpm. The values of rate of incorporation are calculated to be 0.026, 0.009 and 0.005 for 10 wt%, 20wt% and 25 wt% respectively at 10 rpm. Figure 12 shows the same first order kinetics as observed in Figure 4.

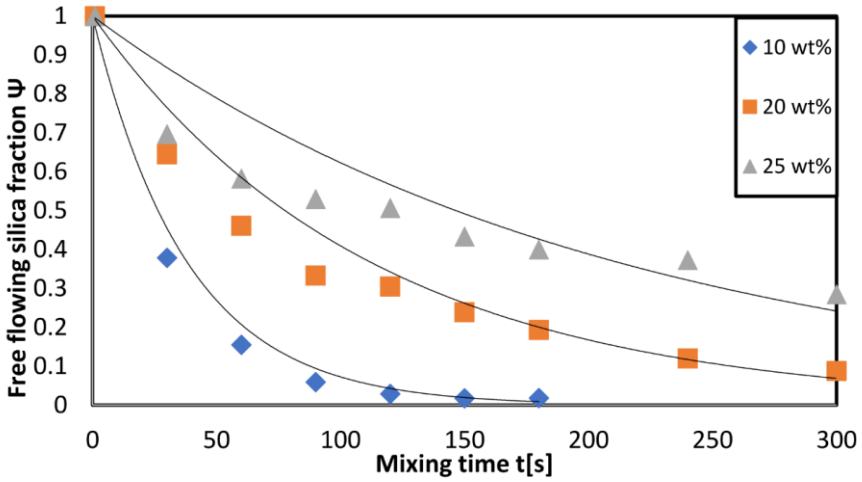

Figure 12. Time evolution of free silica fraction at different silica loads at 10 rpm

After decomposition of the PSD (see procedure in section 1B), the weight fractions x^A and x^B can be calculated and plotted against the mixing time. Figure 13 shows that x^A and x^B increase when the initial load x_0 decreases. This is confirmed in Figure 14 which shows that the particle size reduction is almost linear and more effective at low volume fraction. This suggests that there is more fragmentation of silica particles when the initial silica concentration is lower**.** Indeed, in the case of low initial loading, the characteristic size of the dry silica phase is lower. Shear is thus homogeneous over all the silica phase and granular phase reorganization is promoted. However, in the case of higher initial loading, when the characteristic size of silica phase increases, shear banding could happen that localize shear at silica/rubber interface. As a consequence, shear is not homogeneous in the silica phase and so do the fragmentation. That could explain the slower kinetics.

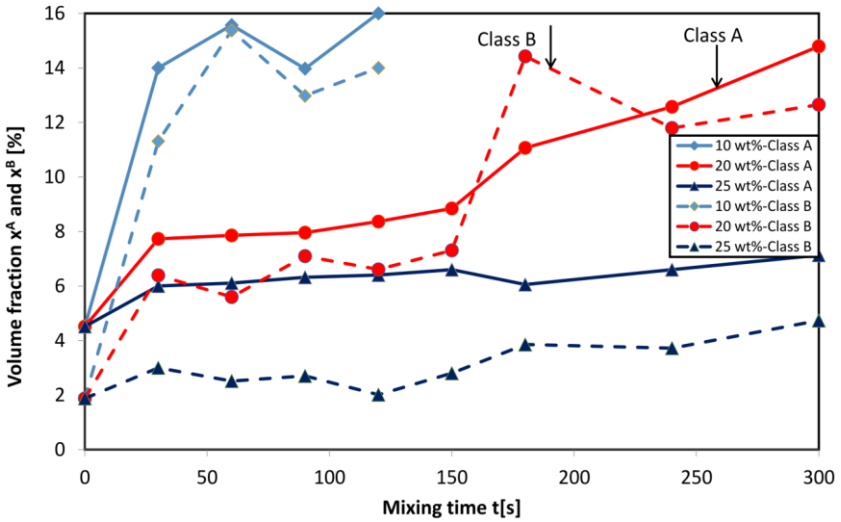

Figure 13. Time evolution of class A (solid line) and class B (dotted line) volume fractions for x_0=10, 20 and 25 wt% at ω=10 rpm

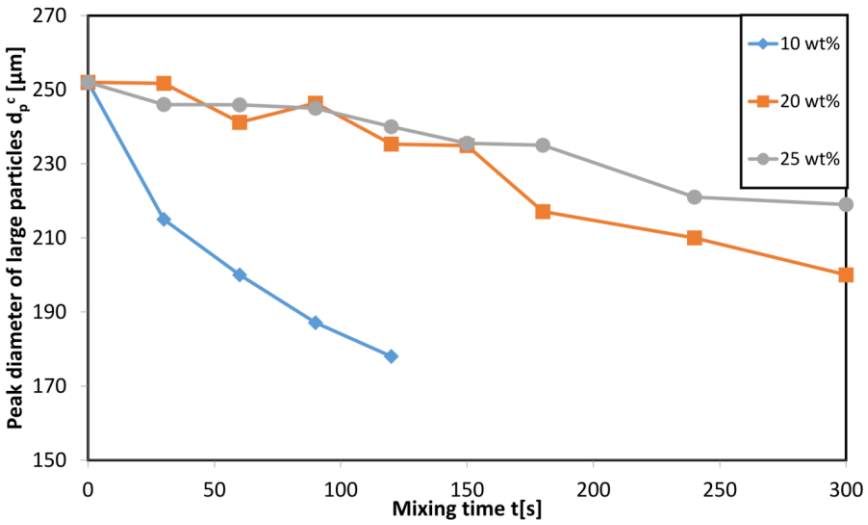

Figure 14. Peak diameter of free large particles (class C) as a function of mixing time for x_0=20 wt% and ω=10 rpm

4.2. Silica embedded in SBR

The X-Ray tomography followed by image analysis enables the determination of the equivalent diameter for every silica particle over 25 µm embedded in SBR. Figure 15 shows the cumulative frequency distribution after various mixing times at 10 rpm. It shows that no silica particles remain above 200 µm, which means that silica particles embedded in SBR are fragmented. To understand the fragmentation better from Figure15, the median diameters are computed and plotted on Figure 16.

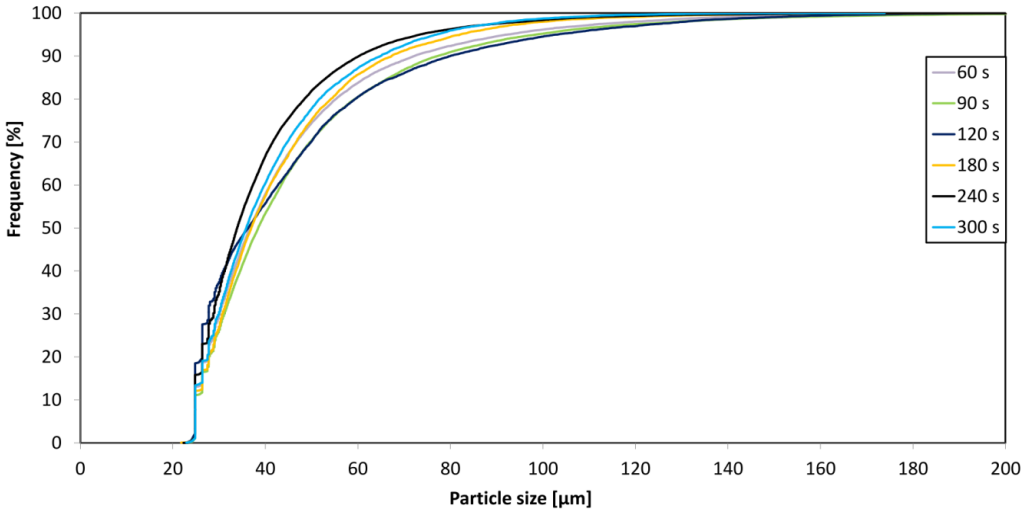

Figure 15. Cumulative Frequency Distribution of silica embedded in SBR

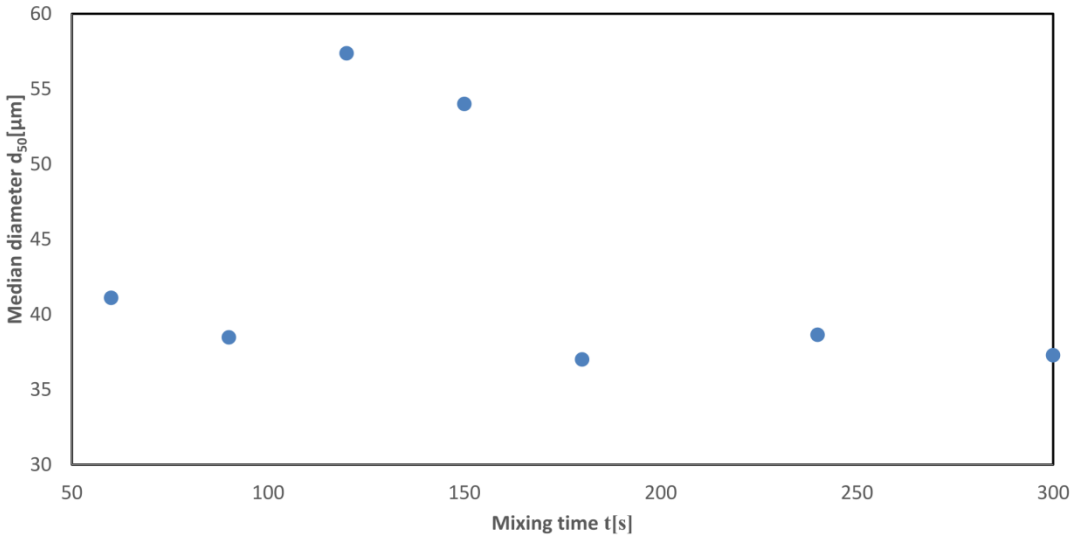

Figure 16. Median diameter of silica particles embedded in SBR

Figure 16 clearly shows that the size of the silica particles falls between 30 and 60 µm, indicating that these particles have clearly ruptured. Our experiments show that the incorporated particles are not the original 200 µm raw micro-beads which are fragile objects. Indeed, by performing experiments on silica sandwiched between SBR using counter rotating shear cells, Boudimbou[27] et al showed that silica Z1165 MP resulted in rupture mechanism for stresses over 200 kPa. Thus, it is clear that the indentation force into SBR required for incorporation is higher than the critical stress for pristine microbead breakage. Thus, only smaller particles (~30-60 µm) resulting from erosion in the dry granular phase can be incorporated without breaking. Once embedded in the rubber phase, the classical dispersion mechanisms can now proceed.

5. Conclusion

To understand the global process for dispersion of silica into SBR, knowledge of the initial stage of mixing is very important. How silica behaves under various mechanisms (shearing, compression, elongation) determines the appropriate industrial process required for homogenous distribution of filler particles within elastomers.This article emphasizes on understanding the incorporation stage using shear forces. Firstly, an experimental method is established to analyze both free silica and silica embedded in SBR. The PSD of free silica is determined using laser granulometry, while silicainside the SBR is analyzed using X-Ray Tomography. We have shown that the amount of classes A and B particles increase with mixing time and that the incorporation rate follows a first order dynamics and increases proportionally to the square root of the rotational speed. Considerable size reduction was observed for both types of silicas, which are mainly due to shear forces inside the internal mixer. For free silica, the maximum

particle size (d_p^c) reduction is around 31% suggests an erosion mechanism.

Acknowledgement:

This study was carried out within the framework of OSUM project, FUI AAP23, funded by BPiFrance. Special thanks are addressed to Bruno Dratz, Jean-Marc Gonnet and Pascal Tremblay from Michelin for their initiative, involvement and discussions during this work, as well as for providing material (SBR) for the experiments.

References:

1. E. M. Dannenberg, “The effects of surface chemical interactions on the properties of filler-reinforced rubbers,” *Rubber Chem Technol*. **1975**;48(3):410-444.
2. R. Rauline, “Composition with silica filler, tires having a base of sad compost on and method of preparing the same,” Published online **1993**:1-9.
3. Luginsland HD, Niedermeier W, “New reinforcing materials for rising tire performance demands,” *Rubber World*. **2003**;228(6):34-45.
4. Prasertsri S, Rattanasom N, “Mechanical and damping properties of silica/natural rubber composites prepared from latex system,” *Polymer Testing*. **2011**;30(5):515-526. doi:10.1016/j.polymertesting.2011.04.001
5. Zou H, Wu S, Shen J, “Polymer/Silica Nanocomposites: Preparation, characterization, propertles, and applications,” *Chemical Reviews*. **2008**;108(9):3893-3957. doi:10.1021/cr068035q
6. M.J. Wang, “The role of filler networking in dynamic properties of filled rubber,” *Rubber Chem Technol*. **1999**;72(2):430-448.
7. A. I. Medalia, “Filler aggregates and their effect on reinforcement,” *Rubber Chem Technol*. **1974**;47(2):411-433.
8. Bohin F, Manas-Zloczower I, Feke DL, “Kinetics of dispersion for sparse agglomerates in simple shear flows: Application to silica agglomerates in silicone polymers,” *Chemical Engineering Science*. **1996**;51(23):5193-5204.
9. Bomal Y, Cochet P, Dejean B, Fourré P, Labarre D, “Une silice de nouvelle génération pour pneumatiques,” *L’Actualité chimique (Paris 1973)*. **1996**;(1):42-48.
10. Boudimbou I, Peuvrel-Disdier E, Dumas T, et al, “Macrodispersion of amorphous precipitated silica micropearls in an elastomer matrix: Role of silica intrinsic parameters,” In: *International Rubber Conference 2013,*. ; **2013**
11. Nakajima N, “An approach to the modeling of mixing of elastomers,” *Rubber Chemistry and Technology*. **1981**;54(2):266-276.
12. Majesté JC, Vincent F, “A kinetic model for silica-filled rubber reinforcement,” *Journal of Rheology*. **2015**;59(2):405-427. doi:10.1122/1.4906621
13. Kaewsakul W, Sahakaro K, Dierkes WK, Noordermeer JWM, “Optimization of mixing conditions for silica-reinforced natural rubber tire tread compounds,” *Rubber Chemistry and Technology*. **2012**;85(2):277-294. doi:10.5254/rct.12.88935
14. Ramier J, Gauthier C, Chazeau L, Stelandre L, Guy L, “Payne effect in silica-filled styrene-butadiene rubber: Influence of surface treatment,” *Journal of Polymer Science, Part B: Polymer Physics*. **2007**;45(3):286-298. doi:10.1002/polb.21033
15. Jin J, “Influence of compounding and mixing on filler dispersion and curing behavior of silica compounds,” Published online **2020**.
16. Bolen WR, Colwell RE, “Intensive mixing,” *Soc Plast Eng J*. **1958**;14(8):24-28.
17. Shiga S, Furuta M, “Processability of EPR in an internal mixter (II)—Morphological changes of carbon black agglomerates during mixing,” *Rubber Chemistry and Technology*. **1985**;58(1):1-22.
18. A. Scurati IMZ and DLF, “Influence of powder surface treatment on the dispersion behavior of silica into polymeric materials,” *Rubber Chem Technol*. **2002**;75(4):725-737.
19. Celine Roux, “Caractérisation in-situ des mécanismes de dispersion dela silice dans une matrice élastomère soumise à uncisaillement,” Published online **2008**.
20. Rwei SP, Manas-Zloczower I, Feke . L, “Characterization of Agglomerate Dispersion by Erosion in Simple Shear Flows, *Polym Eng Sci*. **1991**;31(8):558-562.
21. Astruc M, Collin V, Rusch S, Navard P, Peuvrel-Disdier E, “Infiltration of Uncured Elastomers

into Silica Agglomerates," *J Appl Polym Sci*. **2004**;91:3292-3300.
22. Lee HG, Kim HS, Cho ST, Jung IT, Cho CT, "Characterization of solution styrene butadiene rubber (sbr) through the evaluation of static and dynamic mechanical properties and fatigue in silica-filled compound," *Asian Journal of Chemistry*. **2013**;25(9):5251-5256. doi:10.14233/ajchem.2013.f27
23. Solvay Gmbh, "Zeosil Premium Product Overview," Accessed January 14, **2022.** https://www.solvay.ru/ru/binaries/TIRE SOLUTIONS FICHES-177295.pdf.
24. Grosseau P, Dumas T, Bonnefoy O, Barriquand L, Guy L, Thomas G, "Internal structure and fragmentation kinetics of silica granules," In: *AIP Conference Proceedings*. Vol 1542. ; **2013**:1007-1010. doi:10.1063/1.4812104
25. Anne Marie Helmenstine, "How to Calculate Mass Percent Composition," ThoughtCo. Published November 24, 2019. Accessed January 14, **2022.** https://www.thoughtco.com/mass-percent-composition-example-609567
26. Campanelli JR, Gurer C, Rose TL, Varner JE, "Dispersion, temperature and torque models for an internal mixer," In: *Polymer Engineering and Science*. Vol 44. ; **2004**:1247-1257. doi:10.1002/pen.20120
27. Collin V, Roux C, Peuvrel-Disdier E, Characterization of dispersion mechanisms of agglomerated fillers in an elastomer matrix under shear by in-situ observations," *9th Fall Rubber Colloquium*. Published online **2010**:1-5. https://hal-mines-paristech.archives-ouvertes.fr/hal-00847824